Jour. Fac. Sci., Hokkaido Univ., Ser. IV,
vol. 23, no. 2, Aug., 1992, pp. 211-226

PARTITIONING OF THE TRANSITION METALS Mn, Fe, Co, Ni AND Zn BETWEEN ORTHOPYROXENE AND SILICATE MELT: IONIC SIZE EFFECT TO THE PARTITIONING BEHAVIOR

by

Hideo Hashizume* and Yu Hariya,**

(with 7 text-figures and 10 tables)

Abstract

Partition coefficients of Mn^{2+}, Fe^{2+}, Co^{2+}, Ni^{2+}, and Zn^{2+} between orthopyroxene and silicate melt have been determined in the system Mg_2SiO_4-SiO_2-H_2O at pressures of 1 and 3 GPa and at a temperature of 1400°C. The partition coefficient was defined by the ratio of the concentration of an element in orthopyroxene to that of the element in silicate melt. Partition coefficients were plotted on a partition coefficient versus ionic radius (PC-IR) diagram. Partition coefficients were linearly related to ionic radii. However, the partition coefficient of Zn deviated from the linear relationship between partition coefficients and ionic radii. This was called the Zn^{2+} anomaly. However, a partition coefficient versus metal and oxygen (M-O) distance (PC-MO) diagram was depicted instead of a PC-IR diagram. On a PC-MO diagram, partition coefficients were linearly related to M-O distances. An element with a small M-O distance are concentrated in orthopyroxene. The Zn^{2+} anomaly disappeared on PC-MO diagrams. The partitioning behavior between a site (an M1 or M2 site) in orthopyroxene and silicate melt was estimated by using the intracrystalline cation distribution data. These partition coefficients were plotted on both a PC-M(1)O diagram and a PC-M(2)O diagram. The element of a small M(1)-O distance was concentrated in orthopyroxene on the PC-M(1)O diagram. The lines were negative gentle slopes for the PC-M(2)O diagram. Partition coefficients between the M2 site in orthopyroxene and silicate melt were not almost dependent on the M(2)-O distance.

Introduction

Major and trace elements are partitioned between minerals and silicate melt in magma chamber. The partitioning behavior of elements between a mineral and silicate melt has been one of the most fundamental problems in geochemistry and petrology (Leeman and Lindstrom, 1978; Takahashi, 1978; Doyle and Naldrett, 1986; Schmitt *et al.*, 1989, ect.). The factor of controlling the partition behavior is the ionic size, crystal field stabilization energy, covalency and electronegativity, *etc.* (Irving, 1978; Ford *et al.*, 1983; Seifrt *et al.*, 1988, etc.). Matsui *et al.* (1977) mentioned that the ionic radius was one of the most fundamental factors on the partitioning behavior. The partition coefficients of cations with the same valence gave rise to a parabolic curve to the ionic radii. Matsui *et al.*, (1977) and

Contribution from the Department of Geology and Mineralogy, Faculty of Science, Hokkaido University, No. 2067

* National Institute for Research in Inorganic Materials, Tsukuba, 305 Japan.
** Department of Civil Engineering, Hokkaido Institute of Technology, Sapporo, 006 Japan.

Yurimoto and Sueno (1984, 1987) suggested that an element with the ionic radius of the peak position in the parabolic curve was the most suitable to a crystal structure of a mineral. However, the partition coefficient of Zn was deviated from the parabolic curve in the partition coefficient versus ionic radius diagram (Onuma *et al.*, 1968; Matsui *et al.*, 1977; Yurimoto and Sueno, 1984, 1987). They inferred the Zn^{2+} anomaly from Zn^{2+} preference of a tetrahedral coordination to an octahedral coordination. We made the partitioning experiment between orthopyroxene and silicate melt. Trace elements were selected for divalent cations with similar ionic radii (Mn^{2+}, Fe^{2+}, Co^{2+}, Ni^{2+}, Cu^{2+}, and Zn^{2+}). A PC-MO (partition coefficient versus metal and oxygen distance) diagram was proposed to explain the Zn^{2+} anomaly. Further, orthopyroxene had two cation (an M1 and M2) sites. The elements were partitioned among an M1, an M2 site in orthopyroxene and silicate melt. We estimated partition coefficients between an M1 or an M2 site in orthopyroxene and silicate melt.

Experimental method

Six kinds of starting materials were mixtures of MgO, SiO_2, MnO, CoO, NiO, CuO, ZnO, Fe_2SiO_4 (synthetic fayalite) and $Mg(OH)_2$ ($Mg(OH)_2$ was used in wet condition). The experimental conditions were determined on the basis of the system Mg_2SiO_4-SiO_2-H_2O at pressures 1 and 3 GPa and a temperature 1400℃ (Hashizume *et al.*, 1992). Amount of H_2O in the starting materials was checked from the reduction of weight of starting materials by T. G., and chemical compositions of starting materials were checked by EDAX (Akashi DS-130 + EDAX9100) (Table 1). The starting material for the dry condition (NH in Table 1) was also prepared.

The high pressure experiment was made by piston-cylinder high pressure apparatus. The pressure transmitting medium was molten pyrex glass, and the design of the pressure cell was similar to that figured by Hariya and Kennedy (1968).

Table 1 Chemical composition of the starting materials (wt %).

	E	F	D′	E′	NF	NH
MgO	25.7	22.3	42.5	36.8	21.4	34.1
SiO_2	60.9	67.7	39.5	49.1	68.5	57.1
MnO	0.5	0.5	1.2	1.1	0.4	0.7
FeO	1.1	1.0	1.2	1.1	0.4	0.7
CoO	1.1	1.0	1.3	1.1	0.4	0.7
NiO	1.7	1.5	1.9	1.7	0.9	1.4
CuO	2.5	2.1	4.4	3.4	2.3	3.8
ZnO	2.5	1.1	2.2	1.8	0.9	1.5
H_2O	3.9	3.0	5.8	4.0	4.8	—
	99.9	100.2	100.0	100.1	100.0	100.0

Table 2 Experimental conditions and results of high pressure runs.

Run No.	Sample	Pressure GPa	Temperature ℃	Time hour	Results
013	E	1	1400	3.3	Opx+M
126	F	1	1400	1.0	Opx+M
129	NF	1	1400	1.5	Opx+M
130	NH	1	1560	1.5	Opx+M
303	E	3	1400	1.0	Opx+M
304	E'	3	1400	1.5	Opx+M
307	D'	3	1400	1.5	Ol+Opx+M

Ol ; olivine, Opx ; orthopyroxene, M ; silicate melt.

The sample in a Pt capsule was placed in the center of a graphite tube. The experimental conditions were at pressure of 1 GPa or 3 GPa and at a temperature of 1400℃ in the wet condition, and at a pressure of 1 GPa and a temperature of 1560℃ in the dry condition. The run duration was about 1 to 4 hours. We used the quenching method in recovering the run products. Part of the run product was used for the X-ray powder diffraction and the other part was used for EPMA analysis. The condition of experiment is shown in Table 2.

In the quantitative analysis of EPMA (JEOL 733), operating conditions (accelerating voltage, beam current and counting time for a peak and a back ground) were 15 kV, 20 nA, 20 sec and 5 sec for major elements (Mg and Si), and 25 kV, 28 or 30 nA, 100 sec and 50 sec for minor elements (Mn, Fe, Co, Ni, Cu and Zn). The bean diameter was about 2 to 3 μm and 10 to 30 μm in orthopyroxene and the quenching crystals which showed the silicate melt phase, respectively. The number of analyses was 10 to 50 points for the orthopyroxene and silicate melt phase. The analytical points were determined according to Walker and Agee (1989).

Results

Definition of partition coefficient

The partition coefficient generally represents the ratio of the concentration of the trace element in orthopyroxene to that in silicate melt. For example, the exchange, reaction of a cation between orthopyroxene and silicate melt is represented by

$$Mg^{2+} \text{ in opx} + X^{2+} \text{ in melt} \rightleftarrows X^{2+} \text{ in opx} + Mg^{2+} \text{ in melt} \quad (1)$$

In this case, the partition coefficient is definei by

$$K_D(X/Mg) = (XO/MgO)^{opx}/(XO/MgO)^m \quad (2),$$

where $(XO/MgO)^{opx}$ and $(XO/MgO)^m$ are the ratio of the concentration of XO (X : Mn, Fe, Co, Ni, and Zn) to MgO in orthopyroxene and silicate melt, respectively. If a partition coefficient is larger than 1, an element will be more concentrated in orthopyroxene than MgO in orthopyroxene. If a partition coefficient is

Table 3 Chemical composition of coexisting solid phases and silicate melt phases.

Run No. 013

	Orthopyroxene			Melt		
	A. V.	U. V.	M. E.	A. V.	U. V.	M. E.
MgO	36.39	0.19	0.06	20.75	4.98	0.91
SiO_2	59.57	0.22	0.08	68.76	3.52	0.64
MnO	0.29	0.02	0.01	0.51	0.13	0.02
FeO	0.27	0.04	0.01	0.39	0.08	0.02
CoO	0.35	0.07	0.02	0.19	0.03	0.01
NiO	0.40	0.09	0.03	0.08	0.03	0.01
CuO	0.00	0.00	0.00	0.03	0.09	0.00
ZnO	1.02	0.12	0.04	1.49	0.34	0.07
Total	98.29			92.20		

Atomic ratio

	Opx O= 3	M O= 3
Mg	0.9288	0.5442
Si	1.0200	1.2096
Mn	0.0042	0.0075
Fe	0.0038	0.0057
Co	0.0048	0.0027
Ni	0.0055	0.0011
Cu	0.0000	0.0004
Zn	0.0129	0.0194

Run No. 130

	Orthopyroxene			Melt		
	A. V.	U. V.	M. E.	A. V.	U. V.	M. E.
MgO	36.89	0.32	0.08	31.41	3.71	0.81
SiO_2	60.31	0.25	0.06	62.91	2.13	0.45
MnO	0.42	0.04	0.01	0.95	0.36	0.08
FeO	0.32	0.02	0.01	0.76	0.33	0.07
CoO	0.28	0.03	0.01	0.43	0.05	0.01
NiO	0.68	0.21	0.06	0.38	0.11	0.02
CuO	0.02	0.00	0.00	0.11	0.09	0.02
ZnO	0.76	0.06	0.02	1.37	0.60	0.13
Total	99.68			98.32		

Atomic ratio

	Opx O= 3	M O= 3
Mg	0.9291	0.7989
Si	1.0187	1.0733
Mn	0.0061	0.0139
Fe	0.0046	0.0108
Co	0.0038	0.0060
Ni	0.0093	0.0052
Cu	0.0002	0.0014
Zn	0.0095	0.0173

Run No. 126

	Orthopyroxene			Melt		
	A. V.	U. V.	M. E.	A. V.	U. V.	M. E.
MgO	36.74	1.56	0.59	15.08	6.53	1.88
SiO_2	60.42	0.70	0.27	75.99	4.29	1.24
MnO	0.17	0.04	0.02	0.19	0.02	0.01
FeO	0.33	0.14	0.05	0.30	0.03	0.01
CoO	0.52	0.25	0.09	0.16	0.02	0.01
NiO	0.87	0.49	0.18	0.11	0.07	0.02
CuO	0.00	0.00	0.00	0.03	0.09	0.00
ZnO	0.49	0.21	0.08	0.54	0.11	0.03
Total	99.54			92.40		

Atomic ratio

	Opx O= 3	M O= 3
Mg	0.9205	0.3843
Si	1.0253	1.2989
Mn	0.0024	0.0027
Fe	0.0047	0.0043
Co	0.0071	0.0022
Ni	0.0117	0.0014
Cu	0.0001	0.0005
Zn	0.0061	0.0068

Run No. 303

	Orthopyroxene			Melt		
	A. V.	U. V.	M. E.	A. V.	U. V.	M. E.
MgO	33.69	0.97	0.43	21.26	5.88	2.08
SiO_2	58.74	0.20	0.09	63.31	5.92	2.09
MnO	0.37	0.04	0.02	0.66	0.16	0.06
FeO	0.66	0.08	0.04	0.80	0.23	0.08
CoO	0.92	0.25	0.11	0.42	0.13	0.05
NiO	1.33	0.38	0.17	0.31	0.12	0.04
CuO	0.05	0.03	0.02	0.01	0.01	0.00
ZnO	1.71	0.12	0.05	2.20	0.49	0.17
Total	96.47			88.97		

Atomic ratio

	Opx O= 3	M O= 3
Mg	0.8776	0.5877
Si	1.0264	1.1742
Mn	0.0055	0.0104
Fe	0.0097	0.0124
Co	0.0128	0.0062
Ni	0.0187	0.0046
Cu	0.0006	0.0002
Zn	0.0221	0.0301

Run No. 129

	Orthopyroxene			Melt		
	A. V.	U. V.	M. E.	A. V.	U. V.	M. E.
MgO	36.07	0.32	0.07	14.79	7.75	1.29
SiO_2	59.98	0.33	0.08	78.38	6.33	1.06
MnO	0.24	0.01	0.003	0.32	0.06	0.01
FeO	0.26	0.02	0.005	0.42	0.05	0.08
CoO	0.31	0.01	0.003	0.26	0.07	0.01
NiO	1.32	0.14	0.03	0.34	0.12	0.02
CuO	0.03	0.01	0.00	0.19	0.04	0.01
ZnO	0.69	0.06	0.01	0.89	0.16	0.03
Total	98.90			95.59		

Atomic ratio

	Opx O= 3	M O= 3
Mg	0.9164	0.3661
Si	1.0224	1.3011
Mn	0.0036	0.0046
Fe	0.0038	0.0058
Co	0.0042	0.0034
Ni	0.0182	0.0046
Cu	0.0004	0.0024
Zn	0.0087	0.0109

Run No. 304

	Orthopyroxene			Melt		
	A. V.	U. V.	M. E.	A. V.	U. V.	M. E.
MgO	36.17	0.35	0.10	31.33	2.58	1.05
SiO_2	60.21	0.41	0.12	58.18	5.22	2.13
MnO	0.31	0.05	0.01	0.80	0.42	0.11
FeO	0.22	0.06	0.02	0.71	0.35	0.09
CoO	0.36	0.04	0.01	0.55	0.21	0.05
NiO	1.21	0.10	0.03	0.59	0.28	0.07
CuO	0.12	0.15	0.04	1.63	1.00	0.25
ZnO	0.69	0.06	0.01	1.79	1.09	0.27
Total	99.29			95.58		

Atomic ratio

	Opx O= 3	M O= 3
Mg	0.9154	0.8349
Si	1.0221	1.0401
Mn	0.0045	0.0122
Fe	0.0032	0.0106
Co	0.0049	0.0078
Ni	0.0174	0.0086
Cu	0.0016	0.0221
Zn	0.0087	0.0235

Run No. 307

	Olivine			Orthopyroxene			Melt		
	A. V.	U. V.	M. E.	A. V.	U. V.	M. E.	A. V.	U. V.	M. E.
MgO	50.87	0.57	0.14	37.49	0.38	0.12	35.99	8.12	2.30
SiO_2	43.46	0.89	0.22	61.22	0.35	0.12	56.34	7.15	1.82
MnO	0.39	0.03	0.01	0.43	0.08	0.02	1.33	0.64	0.18
FeO	0.46	0.03	0.01	0.27	0.03	0.01	0.78	0.33	0.09
CoO	0.77	0.05	0.01	0.33	0.03	0.01	0.41	0.12	0.03
NiO	1.45	0.16	0.04	0.36	0.09	0.03	0.21	0.17	0.04
CuO	0.02	0.01	0.004	0.01	0.01	0.00	0.01	0.01	0.00
ZnO	1.24	0.05	0.01	0.82	0.12	0.04	2.46	1.19	0.35
Total	98.66			100.93			97.53		

Atomic ratio

	Ol O= 4	Opx O= 3	M O= 3
Mg	1.8251	0.9311	0.9444
Si	1.0461	1.0198	0.9916
Mn	0.0080	0.0061	0.0199
Fe	0.0092	0.0038	0.0114
Co	0.0148	0.0044	0.0058
Ni	0.0284	0.0048	0.0030
Cu	0.0003	0.0002	0.0002
Zn	0.0222	0.0101	0.0319

Ol; olivine, Opx; orthopyroxene, M; silicate melt, A. V.; average value, U. V.; unbiased variance, M. E.; mean error.

smaller than 1, an element will be more concentrated in silicate melt than MgO in silicate melt.

We calculated the error of the partition coefficient by a following method.

$$\delta x = u/\sqrt{n} \quad (3),$$

where δx is the mean error and u is the unbiased variance ($u^2 = 1/(n-1)\Sigma(x_i - \bar{x})^2$, where x_i and $\bar{x}$ are chemical composition of the i-th analytical point and the average of the chemical composition, respectively). The n is the number of analytical points. The average value (A. V.), the unbiased variance (U. V.) and the mean error (M. E.) of each run product were shown in Table 3. The error of the partition coefficient was calculated by

$$\delta K_D(X/Mg)^2 = (\delta X/X)^2_{opx} + (\delta X/X)^2_m + (\delta Mg/Mg)^2_{opx} + (\delta Mg/Mg)^2_m \quad (4),$$

where δX and δMg are the mean error of XO and MgO in orthopyroxene and silicate melt, respectively. X and Mg are the averaged composition of XO and MgO in orthopyroxene and silicate melt, respectively. The partition coefficients between orthopyroxene and silicate melt and the error of the partition coefficient were shown in Table 4.

Partitioning between orthopyroxene and silicate melt

The relationship of the partition coefficients between orthopyroxene and silicate melt to ionic radii was depicted in Text-fig. 1. The results of seven experiments were represented in the same figure. The magnitude of the partition coefficient was generally an order of K_D(Ni/Mg), K_D(Co/Mg), K_D(Fe/Mg), K_D(Mn/Mg) and K_D(Zn/Mg). Ni^{2+} was most concentrated in orthopyroxene of all elements. K_D(Zn/Mg), K_D(Fe/Mg), and K_D(Mn/Mg) were almost the same values. Zn^{2+}, Fe^{2+}, Mn^{2+} were similarly concentrated in silicate melt.

Table 4 Partition coefficient (K_D) between orthopyroxene and silicate melt.

Run No.	013		126		129		130	
X	K_D	δK_D	K_D	δK_D	K_D	δK_D	K_D	δK_D
Mn	0.32	0.12	0.37	0.17	0.31	0.19	0.38	0.13
Fe	0.39	0.12	0.45	0.20	0.25	0.18	0.36	0.15
Co	1.05	0.12	1.33	0.22	0.49	0.20	0.55	0.06
Ni	2.85	0.15	3.25	0.32	1.59	0.21	1.52	0.15
Zn	0.39	0.12	0.37	0.22	0.32	0.19	0.47	0.15

Run No.	303		304		307	
X	K_D	δK_D	K_D	δK_D	K_D	δK_D
Mn	0.35	0.13	0.34	0.18	0.31	0.15
Fe	0.52	0.14	0.27	0.19	0.33	0.13
Co	1.38	0.17	0.57	0.14	0.77	0.09
Ni	2.71	0.18	1.78	0.16	1.65	0.21
Zn	0.49	0.12	0.33	0.21	0.32	0.16

δK_D ; error of partition coefficients

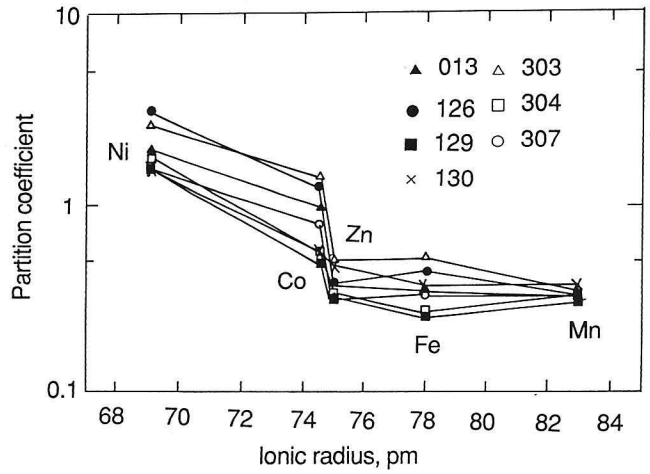

Text-fig. 1 Relationships between partition coefficient and ionic radius (PC-IR diagram) for orthopyroxene and silicate melt system.

Discussion

Comparison with PC-IR diagrams on the dry and wet conditions

In nature, pyroxene is mainly formed in basaltic to rhyolitic rocks. H_2O content in rocks generally increases when SiO_2 content increases in the bulk composition of rocks (Hervig *et al.*, 1989; Clemens, 1984). Therefore, it is important that we compare the partition coefficients for the pyroxene and silicate melt system in the wet condition with those in the dry condition. The difference of conditions (wet and dry) was not apparent in Text-fig. 1 (dry; Run No. 130, wet; other Runs). Therefore, we used a Nernst type partition coefficient ($k(X)=XO^{opx}/XO^{m}$, where XO^{opx} and XO^{m} were the concentration of MgO, MnO, FeO, CoO, NiO and ZnO in orthopyroxene and silicate melt, respectively.). The k(X) is shown in Table 5. A PC-IR diagram is shown in Text-fig. 2. The run products at 1 GPa

Table 5 Nernst type partition coefficient (k) between orthopyroxene and silicate melt at 1 GPa.

Run No.	013		126		129		130	
X	k	δk	k	δk	k	δk	k	δk
Mg	1.75	0.04	2.44	0.13	2.44	0.09	1.18	0.03
Mn	0.57	0.05	0.87	0.10	0.76	0.03	0.44	0.09
Fe	0.69	0.06	1.13	0.16	0.62	0.18	0.42	0.09
Co	1.84	0.08	3.23	0.18	1.20	0.04	0.64	0.04
Ni	5.00	0.10	8.27	0.28	3.85	0.06	1.79	0.10
Zn	0.68	0.06	0.91	0.18	0.78	0.04	0.56	0.10

δk; error of Nernst type partition coefficient

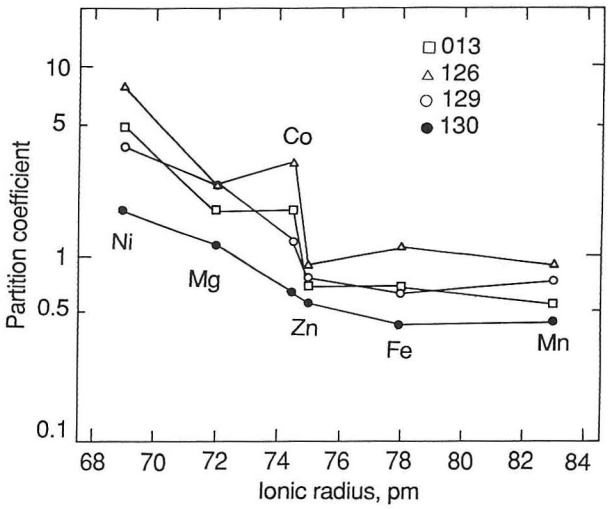

Text-fig. 2 Relationships between Nernst type partition coefficient (k(X)) and ionic radius (PC-IR diagram) for orthopyroxene and silicate melt system.

were selected. Partition coefficients in the dry condition are smaller than those in the wet condition. The difference of the partition coefficients in the dry and wet condition could depend that the melt structure was transformed by the H_2O content.

Comparison with PC-IR diagrams for pyroxene and silicate melt of our system and other systems

The PC-IR diagram for the natural and the experimental system was shown in Text-fig. 3. Ewart *et al.*, (1973) got the partition coefficient between orthopyroxene or clinopyroxene and groundmass for the basaltic andesite to dacite from Late Hunga Ha'apai Fonualei in the Tonga Islands. They analyzed orthopyroxene, clinopyroxene and groundmass with EPMA. They did not analyze ZnO in the samples. Dostal *et al.* (1983) used the sample of xenolith from the Sonfriere volcano, St. Vincent in West India. They analyzed the compositions of the phenocryst and the bulk rock for the atomic absorption. If a small amount of the phenocryst exists in the bulk rock, it will be assumed that the chemical composition of groundmass or glass is almost equal to the bulk composition. Therefore, the partition coefficients were calculated by using their analytical data of phenocryst and the bulk rock composition. Yurimoto and Sueno (1987) showed the partition coefficient between the phenocryst (or megacryst) and glass in the system Boninite. They analyzed them with SIMS. Duke (1976) made the partitioning experiments of each element of Ti, V, Cr, Mn, Co, and Ni between clinopyroxene and silicate melt in the system CaO-Na_2O-MgO-FeO-Al_2O_3-SiO_2. These patterns on the PC-IR diagram were similar to one another. However, K_D(Ni/Mg) in Duke (1976) was smaller than that in the others. He did not investigated this. These results

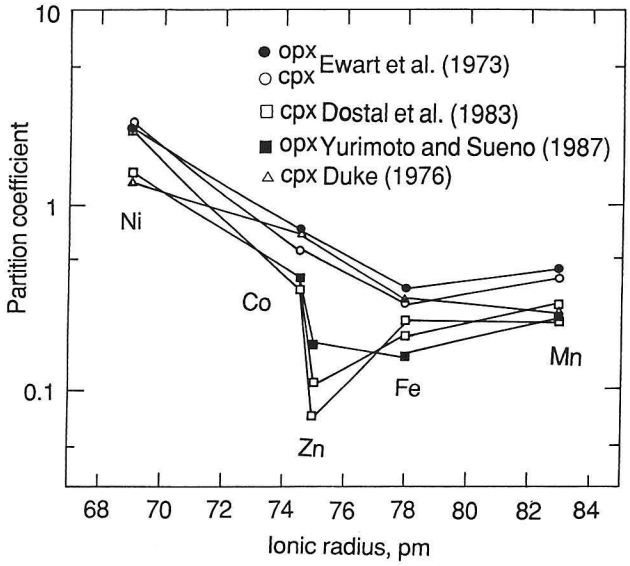

Text-fig. 3 Relationships between partition coefficient and ionic radius (PC-IR diagram) for natural ortho- and clino-pyroxene and groundmass system. (Ewart *et al.*, 1973; Dostal *et al.*, 1983; Duke, 1976; Yurimoto and Sueno, 1987).

showed almost the same tendency. K_D(Zn/Mg) in Yurimoto and Sueno (1987) was larger than that in other workers. The partition coefficients of our result (Text-fig. 1) were almost the same value, as compared with those of other workers. The tendency of PC-IR diagram of our result is particularly similar to that of Yurimoto and Sueno (1987).

Partition coefficients versus metal and oxygen distance diagram

Partition coefficients showed a linear relationship to ionic radii. However, the partition coefficient of Zn deviated from the linear relation. The deviation of Zn was due to the characteristic of Zn^{2+} that preferred a tetrahedral coordination to an octahedral coordination (Yurimoto and Sueno, 1984, 1987; Matsui *et al.*, 1977). The energy of the Zn^{2+} site was compared with that of other cations (Mg^{2+}, Fe^{2+}, and Mn^{2+}) in an octahedral coordination. The energy of Zn^{2+} in the octahedral coordination site was −253.8 kJ/mol (Smyth and Bish, 1988). It was not so different from other cations (Mg, Fe and Mn) in the octahedral coordination site as shown in Table 6 (Smyth and Bish, 1988). These energies show that the degree of doping the cations into the crystal is almost same. Therefore, the anomaly, that K_D(Zn/Mg) is smaller than

Table 6 Electrostatic site energy (kJ/mol) for Mg^{2+}, Fe^{2+}, Mn^{2+} and Zn^{2+} in the octahedral site of carbonate.

	Site energy
Mg	−255.2
Fe	−253.8
Mn	−241.1
Zn	−253.8

other partition coefficient, will be due to other factor without the preference of the tetrahedral coordination to the octahedral coordination. Zn^{2+} has both an ionic and a covalent bonding. Therefore, the metal and oxygen (M-O) distances of orthopyroxene were adopted, because an M-O distance was a parameter showing the bonding state between a metal cation and an oxygen anion. We propose the use of the partition cofficient versus metal oxygen (PC-MO) diagram rather than the PC-IR diagram.

PC-MO diagram for the orthopyroxene and silicate melt system

The M(1)-O and M(2)-O distances for the end members ($MgSiO_3$, $CoSiO_3$, $FeSiO_3$ and $ZnSiO_3$) of orthopyroxenes were shown in Table 7 (M(1) and M(2) were the metal cation in the M1 and M2 site, respectively.). However, $NiSiO_3$ and $MnSiO_3$ do not build an orthopyroxene structure. Therefore, an Mn-O distance in orthopyroxene was employed the analytical data of the solid solution $(Mg_{0.925}Mn_{0.075})SiO_3$ by Hawthorne and Ito (1978). An Ni-O distance was not obtained at all. The Ni(1)-O distances was estimated in Ni-orthopyroxene from the M(1)-O distance in clinopyroxene. M(1) sites in Mg-, Co-, and Fe-orthopyroxenes (Pbca structure) are linearly related to Mg-, Co-, and Fe-clinopyroxene (C2/c structure), as shown in Text-fig 4. Therefore, we could estimate the Ni-O distance of the M(1) site in orthopyroxene (the solid square in Text-fig. 4). However, Ni(2)-O distance were not estimated at all.

Table 7 Average metal-oxide distance (pm) of ortho- and clinopyroxenes. M(1) and M(2) are the average values of six M(1)-O- and six M(2)-O distances. A. V. is the average value of M(1)-O and M(2)-O distances.

Orthopyroxene

	M(1)	M(2)	A. V.	Reference
Mg [1)]	207.8	215.1	211.45	Sasaki and Takeuchi (1982)
Mn	212.1	229.2	220.65	Hawthorne and Ito (1978)
Fe	213.5	222.3	217.9	Sasaki and Takeuchi (1982)
Co	210.3	218.2	214.25	Sasaki and Takeuchi (1982)
Ni	207.25	—	—	Our estimation
Zn	212.8	226.5	219.65	Morimoto *et al.* (1975)

Clinopyroxene

	M(1)	Reference
Mg	207.7	Cameron and Papike (1981)
Mn	217.3	Cameron and Papike (1981)
Fe	213.0	Cameron and Papike (1981)
Co	210.2	Cameron and Papike (1981)
Ni	207.2	Cameron and Papike (1981)
Zn	214.5	Cameron and Papike (1981)

1) Sample $(Mg_{0.925}Mn_{0.075})SiO_3$

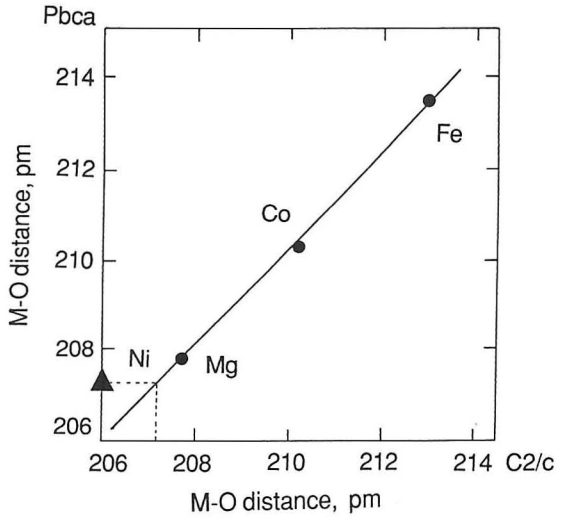

Text-fig. 4 Linear correlation for M(1)-O distances of orthopyroxenes (Pbca structure) and those of clinopyroxene (C2/c structure). The solid triangle is the estimated Ni(1)-O distance.

The PC-MO diagram was shown in Text-fig 5. M-O distances are the average of M(1)-O and M(2)-O distances. K_D(Ni/Mg) was absent in this figure, because we did not understand the average Ni-O distance. A negative slope was shown in Text-fig 5. K_D(Fe/Mg) and K_D(Mn/Mg) had almost the same values. The Zn^{2+} anomaly did not appear. Therefore, the Zn^{2+} anomaly on the PC-IR diagram was an apparent anomaly.

Application of intracrystalline cation distribution in orthopyroxene to the partitioning behavior

A trace element will be partitioned among an M1, an M2 site in orthopyroxene

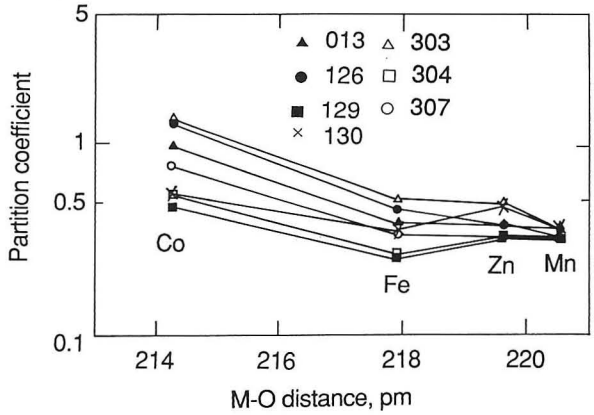

Text-fig. 5 Relationships between partition coefficient and metal and oxygen distance (PC-MO diagram) for orthopyroxene and silicate melt system.

and the silicate melt. We attempted to get a partition coefficient between an M1 site and silicate melt, and between an M2 and silicate melt. The shapes of the two sites in orthopyroxene are different. Therefore, we assumed that the concentration of the trace element in an M1 site was different from that in an M2 site. However, the concentration of the trace element in orthopyroxene was too small to determine the concentration of a trace element in an M1 and M2 sites by the crystal structure analysis. We determined the concentration of the trace element in the M1 and M2 site from the total concentrations of trace elements in orthopyroxene by means of the intracrystalline cation distribution data.

The distribution coefficient in the intracrystalline cation exchanging reaction between an M1 and M2 site is defined by

$$K_D^{M1/M2}(X/Mg)=(A_X^{M1}/A_{Mg}^{M1}/(A_X^{M2}/A_{Mg}^{M2}) \quad (5),$$

where X is Mn, Fe, Co, Ni, or Zn. A_X^{M1} and A_{Mg}^{M1} are the concentration of X and Mg in an M1 site, and A_X^{M2} and A_{Mg}^{M2} are that of X and Mg in an M2 site in orthopyroxene, respectively. The chemical composition of orthopyroxene is defined by $(Mg_{1-Q}X_Q)SiO_3$. A_X^{M1} is defined by P. Then, we will get the other site occupancy ratio. That is to say, $A_X^{M1}=P$, $A_{Mg}^{M1}=1-P$, $A_X^{M2}=2Q-P$ and $A_{Mg}^{M2}=1-2Q+P$ (Akamatsu *et al.*, 1988). The distribution coefficient $K_D^{M1/M2}(X/Mg)$ is rewritten by

$$K_D^{M1/M2}(X/Mg)=P(1-2Q+P)/(1-P)(2Q-P) \quad (6).$$

Q is the concentration of the trace element in the crystal as shown in Table 3 (atomic ratio). The data (A_X^{M1}, A_X^{M2}, A_{Mg}^{M1}, A_{Mg}^{M2}, and $K_D^{M1/M2}(X/Mg)$) of the intracrystalline cation distribution were listed in Table 8. We calculated the concentrations of trace elements in the M1 and M2 site in orthopyroxene using equation (6) from Table 3 and 8. The ratio of the M1 or M2 site of Mg was obtained by subtracting the total site occupancy ratio of trace elements (Mn, Fe, Co, Ni, and Zn) in the M1 and M2 site from the total site number (=1). The concentrations of Mg in the M1 and M2 site would be calculated by using the atomic ratio in Table 3 from the ratio of the M1 and M2 site of Mg. The concentration ratios of an M1 and M2 sites in orthopyroxene in our experiment were shown in Table 9. The concentratinos of trace elements in silicate melt were converted the atomic ratio (O=3), because the concentrations of the M1 and M2 site were shown by the

Table 8 Site occupancy ratio and intracrystalline cation distribution coefficient on orthopyroxenes.

Site occupancy (atomic ratio)								
element	M 1	M 2	element	M 1	M 2	$K_D^{M1/M2}$	Temp. °C	Reference
Mg	0.986	0.924	Mn	0.016	0.076	0.197	800	Saxena *et al.* (1989)
Mg	0.930	0.646	Fe	0.054	0.267	0.140	800	Saxena *et al.* (1989)
Mg	0.735	0.525	Co	0.265	0.475	0.398	—	Ghose *et al.* (1976)
Mg	0.789	0.831	Ni	0.211	0.169	1.315	—	Ghose *et al.* (1976)
Mg	0.933	0.617	Zn	0.067	0.383	0.116	—	Ghose *et al.* (1976)

Table 9 Site occupancies (concentration ratio) of an M1 and an M2 sites in orthopyroxene.

Run No.	013		126		129		130	
site	M1	M2	M1	M2	M1	M2	M1	M2
Mg	0.4684	0.4604	0.4630	0.4575	0.4608	0.4556	0.4681	0.4610
Mn	0.0007	0.0035	0.0004	0.0020	0.0006	0.0030	0.0010	0.0051
Fe	0.0005	0.0033	0.0006	0.0041	0.0005	0.0033	0.0006	0.0040
Co	0.0014	0.0034	0.0020	0.0051	0.0012	0.0030	0.0011	0.0027
Ni	0.0031	0.0024	0.0066	0.0051	0.0103	0.0079	0.0053	0.0040
Zn	0.0013	0.0116	0.0006	0.0055	0.0009	0.0078	0.0010	0.0085

Run No.	303		304		307	
site	M1	M2	M1	M2	M1	M2
Mg	0.4459	0.4317	0.4605	0.4549	0.4694	0.4616
Mn	0.0009	0.0046	0.0007	0.0038	0.0010	0.0051
Fe	0.0013	0.0084	0.0004	0.0028	0.0005	0.0033
Co	0.0037	0.0091	0.0014	0.0035	0.0013	0.0031
Ni	0.0106	0.0081	0.0099	0.0075	0.0027	0.0021
Zn	0.0023	0.0201	0.0009	0.0078	0.0010	0.0089

Table 10 Partition coefficient between a site in orthopyroxene and the silicate melt.

Run No.	013		126		129		130	
	M1/liq	M2/liq	M1/liq	M2/liq	M1/liq	M2/liq	M1/liq	M2/liq
Mn	0.11	0.54	0.12	0.62	0.10	0.52	0.12	0.64
Fe	0.10	0.68	0.12	0.80	0.07	0.46	0.09	0.64
Co	0.60	1.49	0.75	1.95	0.28	0.71	0.31	0.78
Ni	3.27	2.58	3.91	3.06	1.78	1.38	1.74	1.33
Zn	0.08	0.71	0.07	0.68	0.07	0.58	0.10	0.85

Run No.	303		304		307	
	M1/liq	M2/liq	M1/liq	M2/liq	M1/liq	M2/liq
Mn	0.11	0.60	0.10	0.57	0.10	0.52
Fe	0.14	0.92	0.07	0.48	0.09	0.59
Co	0.79	2.00	0.33	0.82	0.45	1.09
Ni	3.04	2.40	2.09	1.60	1.81	1.43
Zn	0.10	0.91	0.07	0.61	0.06	0.57

atomic ratio. The partition coefficients between an M1 site and silicate melt ($K_D^{M1/liq}(X/Mg)=(A_X/A_{Mg})^{M1}/(A_X/A_{Mg})^{liq}$), and between an M2 site and silicate melt ($K_D^{M2/liq}(X/Mg)=(A_X/A_{Mg})^{M2}/(A_X/A_{Mg})^{liq}$) were obtained as shown in Table 10.

Partitioning between an M1 site in orthopyroxene and silicate melt and

between an M2 site in orthopyroxene and silicate melt

The PC-MO diagrams between an M1 site in orthopyroxene and silicate melt, and between an M2 site in orthopyroxene and silicate melt, were depicted in Text-figs. 6 and 7, respectively. There was a bend in the line at $K_D^{M1/liq}$(Mn/Mg) as shown in Text-fig. 6. The line from $K_D^{M1/liq}$(Ni/Mg) to $K_D^{M1/liq}$(Mn/Mg) was steep gradient. $K_D^{M1/liq}$(Mn/Mg), $K_D^{M1/liq}$(Zn/Mg) and $K_D^{M1/liq}$(Fe/Mg) had almost equal values. Ni^{2+} was concentrated in an M1 site in orthopyroxene. Other elements were concentrated in silicate melt. $K_D^{M2/liq}$(Ni/Mg) was not shown in Text-fig. 7,

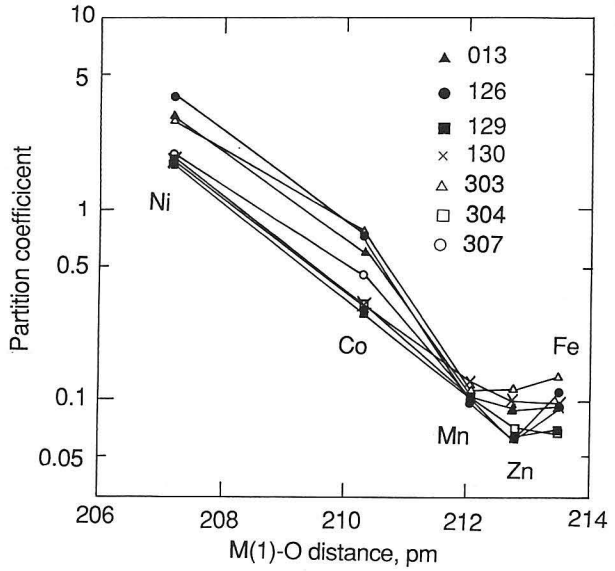

Text-fig. 6 Relationships between partition coefficient and M(1)-O distance (PC-M(1)O diagram) for M1 site in orthopyroxene and silicate melt system.

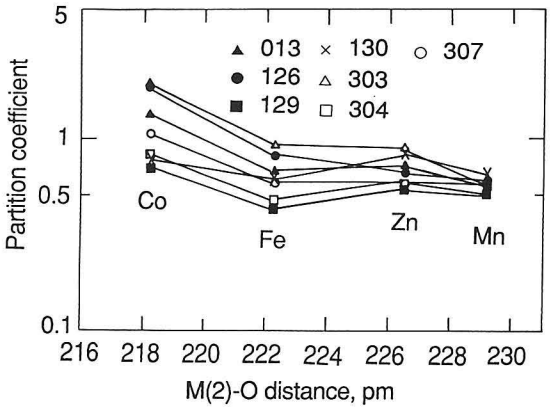

Text-fig. 7 Relationships between partition coefficient and M(2)-O distance (PC-M(2)O diagram) for M2 site in orthopyroxene and silicate melt system.

because Ni(2)-O distance was not estimated. $K_D^{M2/liq}$(Ni/Mg) were larger than the other partition coefficients on each run (Table 10). It was expected that the line had a negative slope from $K_D^{M2/liq}$(Ni/Mg) to $K_D^{M2/liq}$(Fe/Mg). Zn^{2+} anomaly did not appear in Text-fig. 6 and 7. Zn^{2+} anomaly will be apparently anomaly on the PC-IR diagram. In arguing the partitioning behavior, we recommend the PC-MO diagram.

Summary and conclusion

We carried out the partitioning experiments for Mn^{2+}, Fe^{2+}, Co^{2+}, Ni^{2+}, and Zn^{2+} between orthopyroxene and silicate melt. It was attempted to obtain the partition coefficients between a site in orthopyroxene and silicate melt. A partition coefficient versus metal and oxygen (M-O) distance (PC-MO) diagram was proposed instead of a PC-IR diagram. The partition coefficients were almost linearly related to -O distances. Although the Zn^{2+} anomaly exists on a PC-IR diagram, it disappears on a ZC-O diagram. Further, the partition coefficients between the M1 site in orthopyroxene and silicate melt and the M2 site in orthopyroxene and silicate melt were estimated. Partition coefficients between an M1 site in orthopyroxene and silicate melt were almost linearly related to an M(1)-O distance. The tendency of the PC-M(1)O diagram showed negative and steep slopes. Partition coefficients between an M2 site in orthopyroxene and silicate melt were also almost linearly related to an M(2)-O distance. The line slopes were negative and gentle. Zn^{2+} anomaly disappear in PC-MO diagrams. The partition coefficients (k(X)) in the wet condition are larger than those in the dry one. It was found that a k(X) became large in H_2O content. Our experimental partition coefficient (K_D(X/Mg)) were compared with other results of workers on partition coefficient versus ionic radius (PC-IR) diagram. Our results were in good consistent with others.

Acknowledgements

We would like to thank Assoc. Prof. T. Kikuchi and Dr. H. Miura of Hokkaido University for their encouragements, suggestions and discussions during this work.

References

Akamatsu, T., Fujino, K. Kumazawa, M., Kato, M., Sawamoto, H. and Yamanaka, T., 1988. Pressure and temperature dependence of cation distribution in Mg-Mn olivine. *Phys. Chem. Mineral.*, 16: 105-113.

Cameron, M. and Pappas, J. J., 1981. Structure and chemical variations in pyroxenes. *Am. Mineral.*, 66: 1-50.

Clemens, J. D., 1984. Water contents of silicic to intermediate magmas. *Lithos*, 17: 273-287.

Dostal, J. and Dupuy, C., Carron, J. P., LeGuen de Kerneizon, M. and Maury, R. C., 1983. Partition coefficients of trace elements: application to volcanic rocks of St. Vincent, West Indies. *Geochim. Cosmochim. Acta*, 47: 525-533.

Doyle, C. D. and Naldrett J. A., 1986. Ideal mixing of divalent cations in mafic magma and its effect on the solution of ferrous oxide, *Geochim. Cosmochin. Acta*, 50: 435-443.

Duke, J. M., 1976. Distribution of the period for transition elements among olivine, calcic clinopyroxene and mafic silicate liquid: experimental results. *J. Petrol.*, 17: 499-521.

Ewart, A., Bryan, W. B. and Gill, J. B., 1973. Mineralogy and Geochemistry of the younger volcanic islands of Tonga, S. W. Pacific. *J. Petrol.*, 14: 429-465.

Ford, C. E., Russell, D. G., Craven, J. A. and Fisk, M. R., 1983. Olivine-liquid equilibria: Temperature, pressure and composition dependence of the crystal/liquid cation partition coefficients for Mg, Fe^{2+}, Ca and Mn. *J. Petrol.*, 24: 256-265.

Ghose, S., Wan, C., Okamura, F. P., Ohashi, H. and Weidner, J. R., 1975. Site preference and crystal chemistry of transition metal ionic in pyroxenes and olivines. *Acta Cryst.*, A31, Suppl.: S76.

Hariya, Y. and Kennedy, G. C., 1968. Equilibrium study of anorthite under pressure an high temperature. *Am. J. Sci.*, 266: 193-203.

Hashizume, H., Irifune, T. and Hariya, Y., 1992. Melting relations in the sysmem Mg_2SiO_4-SiO_2-H_2O up to 3 GPa. *Mineral. J.*, (submitted).

Hawthorne, F. C. and Ito, J. 1978. Refinement of the crystal structures of $(Mg_{0.776}Co_{0.224})SiO_3$ and $(Mg_{0.925}Mn_{0.075})SiO_3$. *Acta. Cryst.*, B34: 891-893.

Hervig, R. L., Dunbar, N., Westrich, H. R. and Kyle, P. R., 1989. Pre-eruptive water content of rhyolitic magmas as determined by ion microprobe analyses of melt inclusions in phenocrysts. *J. Volcan. Geotherm. Res.*, 36: 293-302.

Irving, A. J., 1978. A review of experimental studies of crystal/liquid trace element partitioning. *Geochim. Cosmochim. Acta,* 42: 743-770.

Leeman, W. P. and Lindstrom D. J., 1978. Partitioning of Ni^{2+} between basaltic and synthetic melts and olivines - an experimental study. *Geochim. Cosmochim. Acta,* 42: 801-816.

Matsui, Y., Onuma, N., Nagasawa, H., Higuchi, H. and Banno, S., 1977. Crystal structure control in trace element partition between crystal and magma. *Bull. Soc. fr. Mineral. Crystallogr.*, 100: 315-324.

Morimoto, N., Nakajima, Y., Syono, Y., Akimoto, S. and Matsui, Y., 1975. Crystal structures of pyroxene-type $ZnSiO_3$ and $ZnMgSi_2O_6$. *Acta Cryst.*, B31: 1041-1049.

Onuma, N., Higuchi, H., Wakita, H. and Nagasawa, H., 1968. Trace element partitioning between two pyroxenes and host lava. *Earth Planet. Sci. Lett.*, 5: 47-51.

Sasaki, S. and Takeuchi, Y., 1982. Electron-density distributions of tree orthopyroxene, Mg_2SiO_6, Co_2SiO_6 and Fe_2SiO_6. *Zeit. für Kristal.*, 158: 279-297.

Shannon, R. and Prewitt, C. T., 1969. Effective ionic radii in oxides and fluorides. *Acta Cryst.*, B25: 925-946.

Saxena, S. K., Domanaghetti, M. C., Molin, G. M. and Tazzoli, V., 1989. X-ray diffraction study of Fe^{2+}-Mg order-disorder in orthopyroxene. Some kinetic results. *Phys. Chem. Minerals,* 16: 421-427.

Schmitt, W., Palme, H. and Wänke, H., 1989. Experimental determination of metal/silicate partition coefficients for P, Co, Ni, Cu, Ga, Ge, Mo, and W and some implications for the early evolution of the earth. *Geochim. Cosmochim. Acta,* 53: 173-185.

Seifert, S., O'Neill, H. St. C. and Brey, G., 1988. The partitioning of Fe, Ni and Co between olivine, matal, and basaltic liquid: An experimental and thermodynamic investigation, with: application to the composition of the lunar core. *Geochim. Cosmochim. Acta,* 52: 603-616.

Symth, J. R. and Bish, D. L., 1988. *Crystal structures and cation sites of the rock-forming minerals.* Boston Allen & Union, London, Sydney, Wellington. pp. 1-329.

Takahashi, E., 1978. Partitioning of Ni^{2+}, Co^{2+}, Fe^{2+}, Mn^{2+} and Mg^{2+} between olivine and silicate melts: compositional dependence of partition coefficient. *Geochim. Cosmochim. Acta,* 42: 1829-1844.

Walker, D. and Agee, C., 1989. Partitioning "equilibrium", temperature gradients, and constrains on earth differentiation. *Earth Planet. Sci. Lett.*, 96: 49-60.

Yurimoto, H. and Sueno, S., 1984. Anion cation partitioning between olivine, plagioclase phenocrysts and the host magma: A new application of ion microprobe study. *Geochem. J.*, 18: 85-94.

Yurimoto, H. and Sueno, S., 1987. Anion and cation partitioning between three pyroxenes,

chrome spinel phenocrysts and the host boninite magma : an ion microprobe study. *Geochem. J.*, 21 : 85-104.

(Manuscript received on May 28, 1992 ; and accepted on June 22, 1992)